Development of IRI Models Based on APT Data

José P. Aguiar-Moya, Pablo A. Torres-Linares, Edgar Camacho-Garita, Fabricio Leiva-Villacorta and Luis G. Loría-Salazar

Abstract As with most pavement deterioration models, pavement monitoring is required during long time in order to properly capture deterioration trends. In this sense, roughness modeling, whether based on subjective parameters such as serviceability or indicators such as the International Roughness Index (IRI), requires significant amounts of data on structural pavement distresses such as rutting, patching, and cracking. Consequently, the initial roughness after construction, the evolution of roughness and surface deterioration in time have to be properly documented. Accelerated pavement tests permit an enhanced roughness data generation process. Furthermore, one of the most important factors in determining the future roughness is roughness after construction that can be carefully monitored and measured. Consequently, an IRI model has been developed based on results obtained at the PaveLab facility containing an HVS equipped with dual profile lasers for monitoring roughness along each test section. The model is based on four experimental sections, each of which has been divided into several tracks to make use of the collected data. The model was defined as a function of loss of support, as measured by means of layer moduli, surface rutting, initial IRI and number of load repetitions. Model estimation was based on a random effects model to account for unobserved heterogeneity and using the aforementioned parameters to reduce instrumental variable bias which can occur when using transfer function estimates

J.P. Aguiar-Moya (✉) · P.A. Torres-Linares · E. Camacho-Garita · F. Leiva-Villacorta · L.G. Loría-Salazar
LanammeUCR, CP-11501-2060, San José, Costa Rica
e-mail: jose.aguiar@ucr.ac.cr

P.A. Torres-Linares
e-mail: pablo.torreslinares@ucr.ac.cr

E. Camacho-Garita
e-mail: edgar.camachogarita@ucr.ac.cr

F. Leiva-Villacorta
e-mail: fabricio.leiva@ucr.ac.cr

L.G. Loría-Salazar
e-mail: luis.loriasalazar@ucr.ac.cr

J.P. Aguiar-Moya et al. (eds.), *The Roles of Accelerated Pavement Testing in Pavement Sustainability*, DOI 10.1007/978-3-319-42797-3_52

as proxy for fundamental material properties in the model estimation process. The estimated parameters showed an increase in efficiency, as compared to Ordinary Least Squares estimated parameters.

1 Introduction

The functional performance of a pavement structure can be quantified in terms of smoothness or roughness of the road surface, which in turn are related to ride quality (Arhin et al. 2015). The concept of riding quality was first incorporated in pavement design methodologies as a result of the American Association of State Highway Officials (AASHO) Road Test (AASHO 1962) and was measured in terms of serviceability, which is a subjective measure of how a panel of users perceive the quality of the pavement (Present Serviceability Rating, PSR). Serviceability in turn was related to several distress types found to play a major role in reducing functional performance as follows:

$$PSI = 5.03 - 1.91\log(1 + SV) - 0.01(C + P)^{0.5} - 1.38RD^2 \quad (1)$$

where PSI = present serviceability index (an estimate of the mean panel serviceability rating); SV = slope variance; C = major cracking in feet per 1000 ft^2 area; P represents patching in square feet per 1000 ft^2 area; and RD = average rut depth of both wheel paths in inches measured at the center of a 4 ft span in the most rutted part of the wheel path.

The *PSI* prediction models were later modified to include variables such as rut depth variance and depressions, in order to improve the predicting capabilities of the model (Darter and Barenberg 1976; Al-Omari and Darter 1992).

Because of the subjectivity associated to *PSR*, an effort was performed to develop other measures of pavement functional level. An important aspect regarding *PSR* is that it was previously identified to be highly related to pavement performance and roughness (Carey and Irick 1960). The relationship was later demonstrated by several DOTs when relating their *PSI* measures or local PSR ratings to roughness values measured by different means (Moore et al. 1987).

In the late 1970s, the NCHRP Report 228 related PSI to roughness by means of the International Roughness Index (*IRI*). During the 1980s, *IRI* was adopted by the World Bank as standard measure of roughness in units of in/mi, m/km, or an equivalent unit (Sayers et al. 1986). *IRI* can be measured by several automated equipment, but is typically measured by a laser profiler. Several relationships have been developed by analyzing and comparing *IRI* and *PSI* data. One such example was presented by Paterson (1986) and is structured as a direct nonlinear relationship (IRI measured in inches per mile):

$$PSI = 5\exp(-0.18 \cdot IRI) \tag{2}$$

A similar model was developed by analyzing data from Louisiana, Michigan, New Jersey, New Mexico, Ohio, and Indiana (Al-Omari and Darter 1992):

$$PSI = 5\exp(-0.26 \cdot IRI) \tag{3}$$

All of the previous models were developed by means of Ordinary Least Squares (OLS), under assumptions of normality and no serial correlation. However, with the current widespread use of profilers, which are capable of measuring at high speeds, the need for developing *IRI* models as a function of pavement condition has increased. This is the case of most current pavement design procedures that include a functional failure criteria such as AASHTO's Pavement Design ME, which was originally proposed under NCHRP 1-37A (Von Quintus et al. 2001a, b; Von Quintus and Yau 2001).

1.1 *Current* IRI *Models*

Because of the relatively constant rate of change of *IRI* with time, the current model that was proposed under NCHRP 1-37A consists of a linear function of different distress types and subgrade properties. The initial functional form proposed for *IRI* was as follows,

$$IRI = IRI_0 + \Delta D + \Delta F + \Delta S \tag{4}$$

where IRI_0 corresponds to the initial *IRI* after construction, ΔD is the effect on *IRI* due to different distress types, ΔF is the effect due to frost-heave potential, and ΔS is the effect associated to subgrade swelling potential. In order to identify the parameters to be included in the model as instruments for ΔD, ΔF, and ΔS, stepwise OLS regression was performed in order to derive an initial expression for *IRI* (Von Quintus et al. 2001a; Mirza and Zapata 2003).

The current model included in Pavement Design ME was structurally simplified to account for site specific properties. The model as presented in the Mechanistic-Empirical Pavement Design Guide Manual of Practice (AASHTO 2008) is as follows:

$$IRI = IRI_0 + 0.0150 \cdot SF + 0.400 \cdot FC_{Total} + 0.0080 \cdot TC + 40.0 \cdot RD \tag{5}$$

where *SF* is a site factor that accounts for environmental, subgrade soil properties, and the age of the pavement structure. FC_{Total} corresponds to the area of fatigue cracking: combined alligator, longitudinal, and reflection cracking under the wheel path in feet^2. *TC* is the length of transverse cracking (feet-mile), and RD is the

average rut depth measured in inches. The structural form associated to the site factor is as follows:

$$SF = Age \cdot [0.02003 \cdot (PI + 1) + 0.007947 \cdot (Precip + 1) + 0.000636 \cdot (FI + 1)] \tag{6}$$

where *PI* is the plasticity index of the subgrade soil, *Precip* is average annual rainfall in mm, and *FI* is the average annual freezing index. The previous model parameters were also calibrated based on Long Term Pavement Performance data for the overall United States. The model itself does not directly include local calibration parameters, but the previous can be accounted for in the cracking and rutting transfer equations that are included in the design guide.

However, as per Aguiar-Moya et al. (2011) the model can be improved accounting for several properties of the *IRI* data. Some of the observations on the model are the following: (i) no constant term included in the model. Even though the initial *IRI* is accounted for, a constant term can determine the presence of omitted variable bias. If the constant parameter is significant, then the variables that are being used to predict *IRI* might not be adequate. On the other hand, if the parameter is not significant, it can be adequately removed from the model.

The previous is of importance when considering that the initial IRI used to model (1) is not measured but extrapolated from the *IRI* field data observed up to 15 years after construction. Furthermore, it is noted by the authors that the distress data used for calibrating the model does not necessarily match the time when *IRI* was recorded. In order to account for the previous, Aguiar-Moya et al. (2011) proposed the use of panel data estimation methods that can be used to determine section specific parameters that can readily account for site-specific properties that are not captured by the exogenous factors. One of the proposed model was the following:

$$IRI_{it} = \beta_0 + \beta_1 \cdot SF_{it} + \beta_2 \cdot FC_{Total_{it}} + \beta_3 \cdot TC_{it} + \beta_4 \cdot RD_{it} + u_i + \varepsilon_{it} \tag{7}$$

which consists of a random-effects model where each factor is a function of site "*i*" at time "*t*", β_0 is an average pavement initial condition (representing initial *IRI*), and u_i is a random component of the intercept intended to capture omitted-variable bias that is constant for each pavement section in time. However, further advantage from the data cross-sectional and time series data can be obtained when considering serial correlation: the distress at time "*t*" is related to the distress at time "$t - 1$", and should therefore not be considered as independent.

An alternative approach to modeling IRI has been presented by Lin et al. (2003) and George et al. (1998) where IRI is predicted as a function of different distress types based on the use of Artificial Neural Networks.

1.2 Objective

The objective of this study was to calibrate an *IRI* prediction model using measured profile, rutting, and stiffness data collected from instrumented flexible pavements under accelerated pavement testing conditions.

1.3 Test Sections

The initial set of experiments performed at PaveLab in Costa Rica correspond to 4 structures that were constructed by March 2012 (Fig. 1) (Aguiar-Moya et al. 2012). HVS trafficking on the sections began in July 2013 using a dual 11R22-5 tire, with 90 psi inflation pressure, applying a standardized 40 KN load. The objective of this set of experiments consisted in the structural comparison of typical conditions in the Country: use of granular versus cement-treated bases (CTB), and thin versus thick HMA layers. Table 1 summarizes the thickness and material properties of the analyzed sections. Layer thicknesses were verified by means of Ground Penetrating Radar (GPR) and cores. Initial layer moduli was determined by means of back-calculation based on Falling Weight Deflectometer (FWD) results (Leiva-Villacorta et al. 2015).

The top layer consists of an asphalt concrete (AC) mixture with nominal maximum aggregate size of 19.0 mm with an optimum binder content of 4.9 % by total weight of mixture. The CTB was designed to withstand 35 kg/cm^2 with an

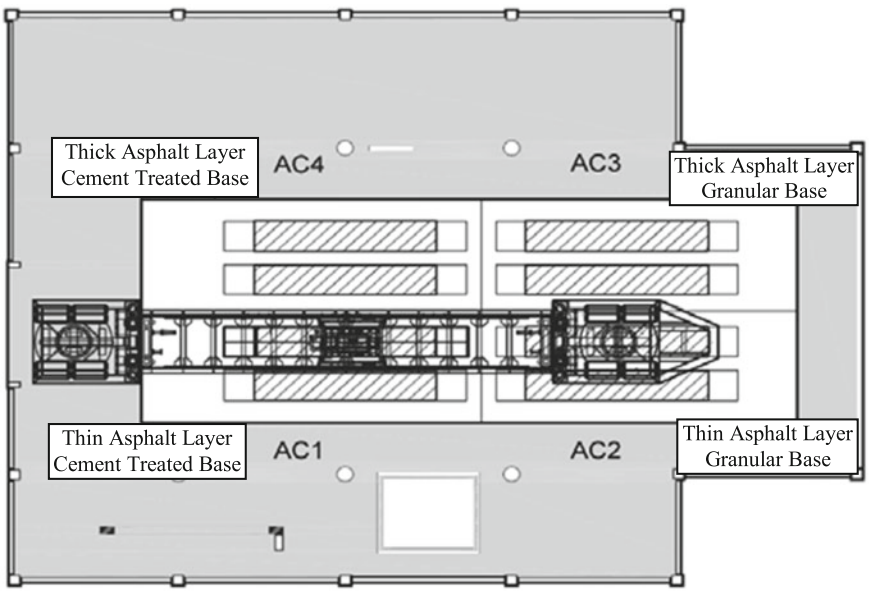

Fig. 1 Test track distribution

Table 1 Test tracks in-place properties

Properties\section	AC1	AC2	AC3	AC4
AC thickness (H1), cm	6.1	6.3	13.2	13.2
Base thickness (H2), cm	21.9	21.2	31.0	24.9
Subbase thickness (H3), cm	30.1	30.1	30.1	30.1
Initial AC modulus (E1) @ 25 °C, MPa	3800	3800	3800	3800
Initial base modulus (E2), MPa	1200	170	170	1200
Initial subbase modulus (E3), MPa	140	140	140	140
Initial subgrade modulus (E4), MPa	70	70	70	70

optimum cement content of 1.7 % by volume of aggregate and with a maximum density of 2013 kg/m^3. The base material and granular subbase were placed at a maximum density of 2217 kg/m^3 with an optimum moisture content of 8.6 %. The subbase material had a CBR of 95 %. Finally, the subgrade material (MH, A-7-5) was constructed for a maximum density of 1056 kg/m^3 with an optimum moisture content of 52 % (typical moisture content in Costa Rica) and CBR of 6.6 %. Both the subgrade and subbase material properties are uniform for all test sections.

1.4 Instrumentation

The measurements were performed using the HVS integrated instrumentation and embedded sensors in all four test sections. HVS onboard instrumentation record the applied load, tire pressure and temperature, position and velocity of the load carriage. Embedded sensors include asphalt strain gauges, pressure cells, multi depth deflectometers (MDDs), and moisture and temperature probes. The HVS was further equipped with a laser profiler that can be used to create a three-dimensional profile of the section and a road surface deflectometer to obtain deflection basins at any location along the test section.

Figure 2 shows the instrumentation array used for the first set of experiments. The asphalt strain gauges were placed at the base/HMA layer interface in the longitudinal and transverse directions. Pressure cells were placed at the subbase/subgrade interface. MDDs were installed at four different depths to cover all four structural layers. The thermocouples were placed at four depths: surface, AC layer mid-depth, at the asphalt strain gauges depth and 5 cm into the base layer. In the case of AC1 and AC4 sections the same gauge array was used while excluding PAST sensors.

Data collection of the 3D profile, strain, pressure, temperature and deflection is performed based on load repetitions. At the beginning of each test, data is obtained at short intervals. After 20,000 load repetitions, data is collected on daily basis. Inspection of fatigue and reflective cracking, friction loss, loss of aggregate-asphalt bond and any other surface damage is performed on daily basis during the HVS daily maintenance work.

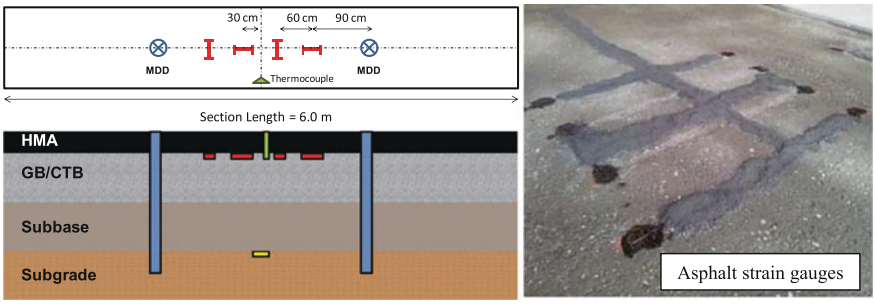

Fig. 2 Sensor array

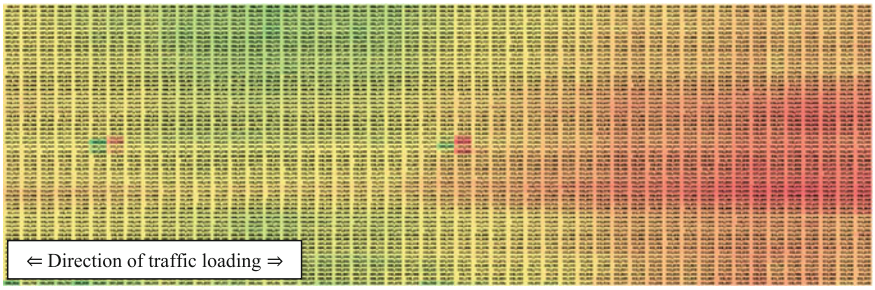

Fig. 3 Test section example profile matrix

The data collected by the two profilers consist of a matrix of information that stores the distance between the sensors and the pavement surface in the longitudinal direction at 4 in intervals and in the transverse direction at every 1 inch. Therefore, each test section is subdivided into 50 subsection in the longitudinal direction and 64 in the transverse direction for a total of 3200 subsections as per Fig. 3.

The IRI was estimated by means of the quarter-car vehicle math model for each of the longitudinal data lines; the transverse measurements are independent. A limitation associated to the IRI estimation is that the length of the section is 6 m, and within this distance the effective measuring distance of the lasers is 5.1 m. Therefore, the IRI corresponds to an average property within the aforementioned distance. The previous differs to IRI measured by means of profilers in the road network since the IRI is reported for a longer section length (50, 100, 200 m). The difference is important since a longer averaging length reduces the impact of outliers or IRI values that deviate significantly from the mean. However, as opposed to network level measurements, the quality of the data or possible outliers could be verified using the 64 subsections for each experiment.

In order to correlate IRI to material deterioration, moduli backcalculation was also performed using multi-depth deflectometers (MDD) data in order to determine the reduction in stiffness that the different material layers are subjected to. Figure 4 shows the increase in deflection and reduction in backcalculated moduli associated

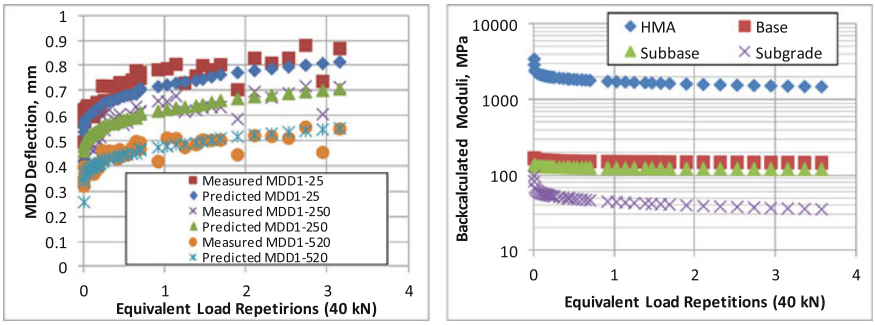

Fig. 4 MDD backcalculated layer moduli for AC3

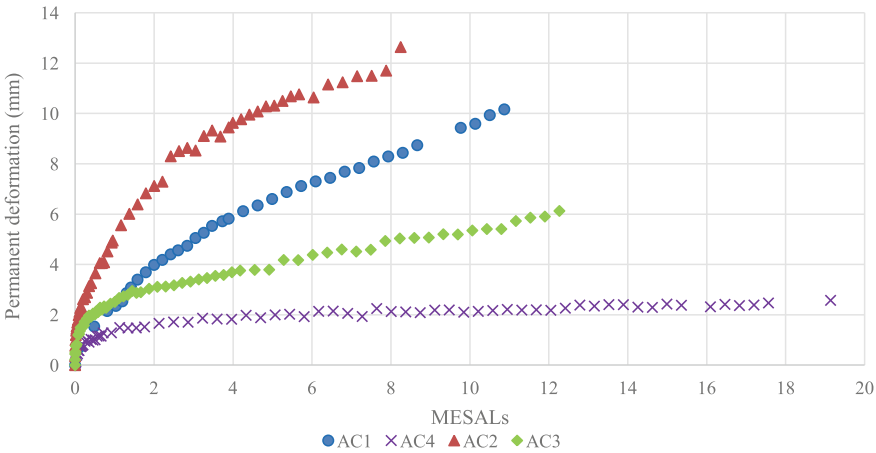

Fig. 5 Average measured permanent deformation

to trafficking for a particular test section. Furthermore, permanent deformation of each test section was also recorded (Fig. 5). It can be noted that the section with least permanent deformation is AC4 (thick HMA layer and CTB). It was also noted that increased thickness in the HMA layer (and no CTB) outperformed the use of a CTB with a thinner HMA layer.

2 APT IRI Data

The average IRI data for the evaluated test sections are shown in Fig. 6. The data indicate that in general, the initial IRI after construction for most sections is in the order of 1 mm/m. The exception corresponds to section AC1 which presented significant construction variability in the CTB and HMA layers, and resulted in higher initial IRI (over 1.7 m/km).

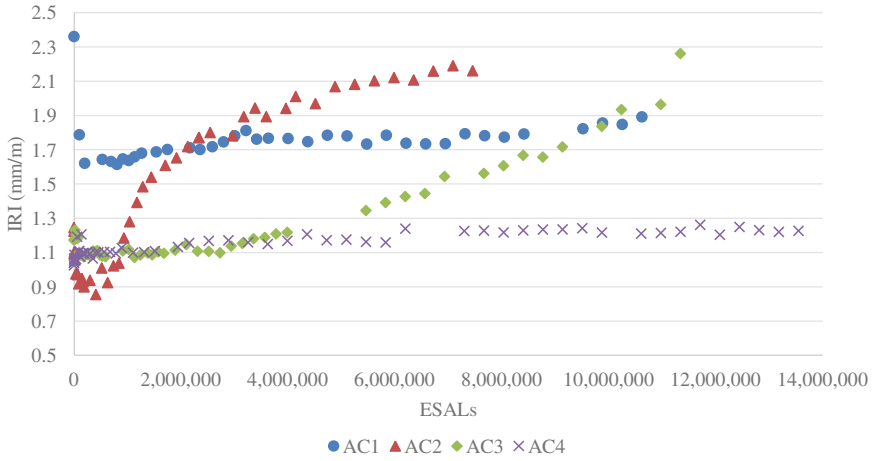

Fig. 6 IRI in different test sections

In general, the IRI data exhibits a linear growth trend. The exception is the AC2 section which corresponds to the weaker structure: thin HMA layer and granular base. The section showed a decreasing rate of IRI growth rate. For the initial 1.5 Million ESAL applications, the section exhibited a higher IRI increase; however, after 1.5 Million ESALs, the IRI increase rate becomes linear.

An additional observation of interest is that the IRI growth rate for sections AC1 and AC4 is similar. This serves as a verification that IRI is highly dependent on roughness of the underlying layers, which for the aforementioned sections is the same (CTB layer underneath HMA). A similar case occurs for sections AC2 and AC3, which correspond to the granular base sections.

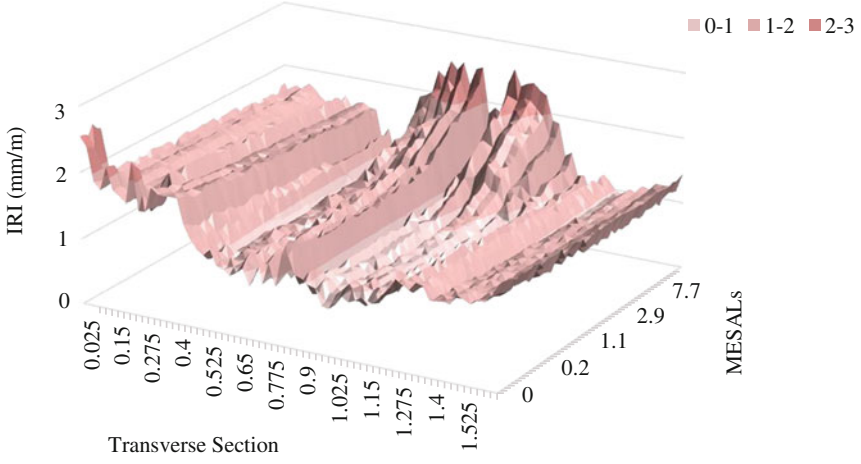

Fig. 7 Variability in IRI for AC3

However, it is important to highlight that the IRI displays considerable variability within each test section (both longitudinal and transverse directions). The degree of variability can be exemplified in Fig. 7. As expected, the area which is subjected to higher trafficking due to wheel wandering initially exhibits lower IRI values but when damage occurs, the IRI rate of increase grows significantly. From the modeling perspective, the previous is important since it suggests that the model will need to account for heteroscedasticity in the data: variability in IRI as a function of trafficking or service life. As such, traditional estimation by means of OLS is inefficient.

3 IRI Model Estimation

An initial *IRI* model was calibrated using multiple linear regression by generalized least squares (GLS), to account for heteroscedasticity. The structural form of the model is the following:

$$\Delta IRI_{it} = \beta_0 + \beta_1 T_i + \beta_2 S_{HMA,it} + \beta_3 S_{B,it} + \beta_4 S_{SB,it} + \beta_5 S_{SG,it} + \beta_6 R_{it} + \beta_7 N_{it} + e_{it} \quad (8)$$

where ΔIRI_{it} corresponds to the change in *IRI* for section "*i*" at time "*t*" in m/Km in reference to initial *IRI* after construction, T represents the initial thickness for the overall pavement structure in mm, S is the stiffness of each pavement layer in MPa at time "*t*", R is the total rutting in mm at time "*t*", N is number of load cycles in ESALs at time "*t*", β_1 thru β_7 are calibration parameters to be estimated, and e_{it} are unobserved factors that are not captured by the model. The estimated parameters are shown in Table 2. Note that the model accounts for the incremental damage in the different layers of the pavement structure.

The previous model attempts to correct for heteroscedasticity in the IRI model because of correlation between the regressors (independent variables) and the error term; however, better predictions of IRI can be obtained when accounting for heterogeneity and the type of data being used in modeling of IRI. In estimating the previous model, all the time series data (performance information for a given pavement section through time) and the cross-sectional data (different pavement sections at any given time) have been combined or pooled together. However, the data corresponds to a panel data set: cross-sectional and time series data (Prozzi and Madanat 2003).

A panel dataset refers to a data type that combines a temporary dimension with another cross-section dimension for each unit of study: pavement sections are monitored through time. Therefore, the bias in the model can be reduced by accounting for unobserved variables that differ from one section to the next, such as material differences, construction variability, or other site-specific variables that do not change over time (heterogeneity).

Table 2 Estimated model parameters

Factor	GLS			RE			FE		
	Coefficient	SE	t-Stat	Coefficient	SE	t-Stat	Coefficient	SE	t-Stat
T	0.0025381	0.0013665	1.86	0.0026736	0.0036325	0.74	–	–	–
S_{HMA}	−0.0001096	0.0000127	−8.64	−0.0002714	0.0000201	−13.5	−0.0003556	0.0000257	−13.86
S_B	0.000037	0.0000379	0.98	−0.0014032	0.0001047	−13.4	−0.0018767	0.0001283	−14.63
S_{SB}	0.0011749	0.0002783	4.22	−0.0004584	0.0002523	−1.82	0.0004147	0.0003104	1.34
S_{SG}	0.001502	0.0003211	4.68	0.0160145	0.0005682	28.18	0.0182281	0.000635	28.71
R	0.0421306	0.004373	9.63	0.0838147	0.0019081	43.93	0.0868718	0.0019247	45.14
N	2.06×10^{-08}	1.90×10^{-09}	10.88	2.79×10^{-08}	1.18×10^{-09}	23.73	2.91×10^{-08}	1.18×10^{-09}	24.68
ΔIRI_{t-1}	–	–	–	0.0026698	0.0004975	5.37	0.0025659	0.0004975	5.16
Intercept	−0.4222819	0.1346159	−3.14	−0.7306446	0.2377246	−3.07	−0.5723572	0.0295232	−19.39

The purpose of modeling based on panel data is to capture the unobservable heterogeneity among the variables and time. The application of this methodology allows the analysis of two important aspects that are part of unobservable heterogeneity: (i) the specific individual effects, which are those that unevenly affect each variable contained in the sample, that directly affects its behavior, and (ii) temporary effects, which are those that equally affect all individual samples but vary over time (Mayorga and Muñoz 2000).

In the panel data models, the time factor was captured by the number of loading cycles (ESAL applications) and the dependent and independent variables are the same that were used to generate the initial GLS model (8). The model includes an auto-recursive [AR (1)] component (at time "t", considers the *IRI* at time "t − 1"). The general form of the proposed model is as follows:

$$\Delta IRI_{it} = \alpha_i + \beta_1 T_i + \beta_2 S_{HMA,it} + \beta_3 S_{B,it} + \beta_4 S_{SB,it} + \beta_5 S_{SG,it} + \beta_6 R_{it} + \beta_7 N_{it} + \beta_8 \Delta IRI_{it-1} + u_i + e_{it} \quad (9)$$

where u_i represents the unobservable effects that differ between samples but not in time, e_{it} refers to the purely random error, and α_i and β_1 thru β_8 are the calibration parameters. ΔIRI_{it-1} corresponds to the change in IRI associated to the previous cycle [AR (1) component].

The model was estimated by means of fixed effects (FE) and random effects (RE) techniques. The fixed effects analysis was performed in order to estimate section specific intercepts (recognizing that omitted variables may lead to changes in the intercepts either over time or among cross-sectional units) and for random effects case, the model intercept is considered as a random variable accounting for differences in test sections associated to heterogeneity. The results are shown in Table 2. Figure 8 shows the predicted values versus observed values for the estimated models.

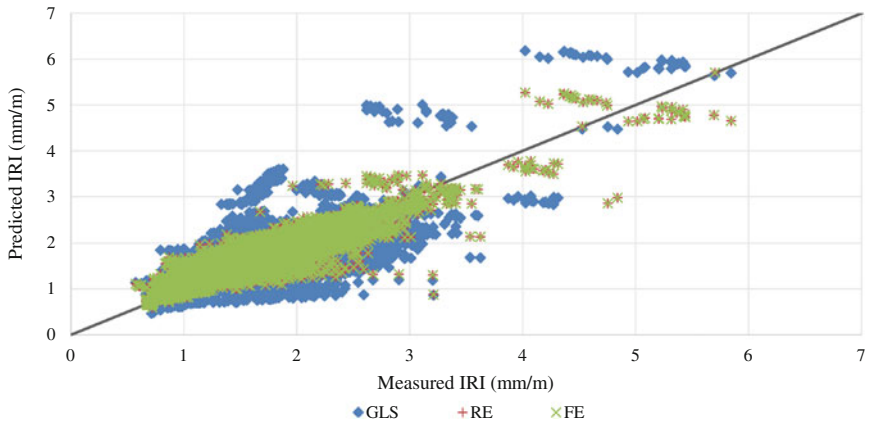

Fig. 8 Predicted versus observed IRI values

Based on the GLS model predictions, when considering heteroscedasticity, the change in IRI can be mostly accounted for by changes in the stiffness of the HMA layer, subbase layer, and subgrade layer; permanent deformation of the pavement structure, and the traffic loading (most significant factor). Therefore, as expected, the change in IRI can be related to the damage induced to the pavement structure as a result of traffic loading: on average 1 Million ESAL applications can be associated to an IRI increase of 0.02 mm/m.

The impact of permanent deformation of the pavement structure is considerable: a 1 mm increase in rut depth can result in an IRI increase of 0.04 mm/m. Therefore, for a permanent deformation failure criteria of 12.5 mm, as a minimum an increase in IRI of 0.53 mm/m is expected, considering no other changes in material or structural properties has occurred. Of slightly less statistical significance is overall pavement thickness. However, based on the GLS model, on average thicker pavement structures can be associated to lower IRI values.

As per Fig. 8, using the panel data models that account for sections specific properties (heterogeneity) improves fit and reduces bias significantly. Because pavement thickness is a particular property of each pavement section, its effect is absorbed by the $\alpha_i + u_i$ sections specific terms. As with the GLS model, changes in material stiffness have an important effect in IRI, however, in contrast to the GLS model, changes in base stiffness have an important effect in predicting IRI: a 1000 MPa change in stiffness can be related to an IRI increase of 0.1 mm/m.

Rut depth and traffic loading also continue to be highly significant factors in explaining changes in IRI. Of special interest is the AR (1): ΔIRI_{it-1} which corresponds to the predicted/measured IRI in the previous time period. Because the factor is significant, it can be concluded that there is correlation between current IRI and IRI deterioration history: changes in IRI in the past have an effect on current

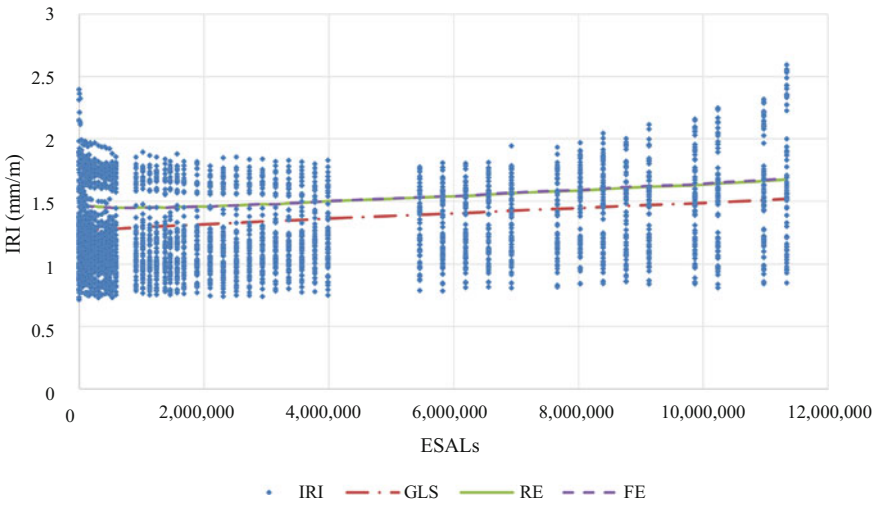

Fig. 9 Predicted IRI values for AC3

IRI. An example of the improvement in model fit using panel data models is shown in Fig. 9 (estimation example for section AC3, similar results obtained for remaining sections). Note that the models including the AR (1) term properly predict the initial reduction in IRI that can be attributed to post compaction of the pavement section.

4 Summary and Conclusions

Models for predicting IRI have been developed based on changes in roughness resulting from APT results on several pavement test tracks. The models have been defined as a function of traffic loading, but are also based on structural distress captured by changes in layer stiffness and permanent deformations of the pavement structure.

Considering current weaknesses in IRI models included in AASHTO's Pavement Design ME, the proposed models improves on efficiency accounting for data heteroscedasticity and attempt to reduce omitted-variable bias because of heterogeneity that is present in the data because of unobserved section-specific variables. The latter can be achieved modeling IRI based on panel data techniques, as opposed to standard OLS methods.

The panel data methods not only improve the models from a theoretical standpoint but also result in changes in the estimated parameters: effect of variables differs between OLS/GLS estimation and panel data estimates. The previous results from the improvement in model consistency (reduction in bias) and efficiency. In general the estimated suggest that changes in stiffness of the different material layers, permanent deformation of the pavement structure, and traffic loading are fundamental in predicting changes in IRI. The previous is expected since pavement distress (rutting and cracking) have been historically identified as having an important effect on IRI. The panel data models with an auto recursive term also suggest that there is significant correlation between current IRI and previous IRI measurements and therefore should be accounted for: IRI history is fundamental in determining future IRI.

Finally, because stiffness data is not always readily available, the authors are currently researching the use of surface deflections as instruments for material stiffness. Deflection data can be easily obtained from PMIS data and can therefore be included in future models.

References

AASHO. (1962). *The AASHO road test*. Special Report 61E. Washington, DC: American Association of State Highway Officials, Highway Research Board.

AASHTO. (2008). *Mechanistic-empirical pavement design guide. A manual of practice.* Washington, DC: American Association of State Highway Officials, Highway Research Board.

Aguiar-Moya, J. P., Corrales-Azofeifa, J. P., Loria-Salazar, L. G., & Elizondo-Arrieta, F. (2012). PaveLab and heavy vehicle simulator implementation at the National Laboratory of Materials and Testing Models of the University of Costa Rica. Advances in pavement design through full-scale accelerated pavement testing.

Aguiar-Moya, J. P., Prozzi, J., & Smit, A. D. F. (2011). Mechanistic-empirical IRI model accounting for potential bias. *Journal of Transportation Engineering, 137*(5), 297–304.

Al-Omari, B., & Darter, M. I. (1992). *Relationships between IRI and PSR, interim report*. Publication No. UILU-ENG-92-2013. Springfield, IL: Illinois Department of Transportation.

Arhin, S. A., Williams, L. N., Ribbiso, A., & Anderson, M. (2015). Predicting pavement condition index using international roughness index in a dense urban area. *Journal of Civil Engineering Research, 5*(1), 10–17.

Carey, W. N. Jr., & Irick, P. E. (1960). *The pavement serviceability performance concept*. Highway Research Board Bulletin 250, Washington, DC.

Darter, M. I., & Barenberg, E. J. (1976). *Zero-maintenance pavements: Results of field studies on the performance requirements and capabilities of conventional pavement*. Report No. FHWA-RD-76-105. Washington, DC: Federal Highway Administration.

George, K. P., El-Rahim, A. M. A., & Shekharan, A. R. (1998). Updates of pavement performance modeling. In: *Third International Conference on Road and Airfield Pavement Technology Proceedings* (pp. 402–4010), Beijing, China.

Leiva-Villacorta, F., Aguiar-Moya, J. P., & Loría-Salazar, L. G. (2015). Accelerated pavement testing first results at the LanammeUCR APT facility. In *Transportation Research Board 94th Annual Meeting Proceedings*, Washington, DC.

Lin, J. D., Yau, J. T., & Hsiao, L. H. (2003) Correlation analysis between international roughness index (IRI) and pavement distress by neural network. In *82th Annual Meeting of the Transportation Research Board Proceedings*, Washington, DC.

Mayorga, M., & Muñoz, E. (2000). *The technique of panel data: A guide for use and interpretation*. Central Bank of Costa Rica, Economic Division, DIE-NT-05-2000, San José, Costa Rica.

Mirza, M. W., & Zapata, C. (2003). *Appendix OO-3: Addendum—Estimation of distress quantities for smoothness models for HMA surface pavements. Guide for mechanistic-empirical design of new and rehabilitated pavement structures*. Washington, DC: National Cooperative Highway Research Program, Transportation Research Board.

Moore, R. K., Clark, G. N., & Plumb, G. N. (1987). Present serviceability-roughness correlations using rating panel data. *Transportation Research Record, 1117*, 152–158.

Paterson, W. D. (1986). *International roughness index: Relationship to other measures of roughness and riding quality*. Transportation Research Record, No. 1084.

Prozzi, J. A., & Madanat, S. M. (2003). Incremental nonlinear model for predicting pavement serviciability. *Journal of Transportation Engineering, 129*(6), 635–641.

Sayers, M. W., Gillespie, T. D., & Paterson, W. D. O. (1986). *Guidelines for conducting and calibrating road roughness measurements*. World Bank Technical Paper 46. Washington, DC.

Von Quintus, H. L., Eltahan, A., & Yau, A. (2001a). *Smoothness models for hot-mix asphalt-surfaced pavements developed from long-term pavement performance program data* (pp 139–156). Transportation Research Record No. 1764.

Von Quintus, H. L., & Yau, A. (2001). *Appendix OO-2: Revised smoothness prediction models for flexible pavement. Guide for mechanistic empirical design of new and rehabilitated pavement structures*. Washington, DC: National Cooperative Highway Research Program, Transportation Research Board.

Von Quintus, H. L., Yau, A., Witczak, M. W., Andrei, D., & Houston, W. N. (2001b). *Appendix OO-1: Background and preliminary smoothness prediction models for flexible pavements. Guide for mechanistic empirical design of new and rehabilitated pavement structures*. Washington, DC: National Cooperative Highway Research Program, Transportation Research Board.